

Analytical expressions for radiatively corrected Higgs masses and couplings in the MSSM *

M. Carena[‡], J.R. Espinosa[§], M. Quirós^{‡ †} and C.E.M. Wagner[‡]

[‡]CERN, TH Division, CH-1211 Geneva 23, Switzerland

[§]Deutsches Elektronen-Synchrotron DESY, Hamburg, Germany

Abstract

We propose, for the computation of the Higgs mass spectrum and couplings, a renormalization-group improved leading-log approximation, where the renormalization scale is fixed to the top-quark pole mass. For the case $m_A \sim M_{\text{SUSY}}$, our leading-log approximation differs by less than 2 GeV from previous results on the Higgs mass computed using a nearly scale independent renormalization-group improved effective potential up to next-to-leading order. Moreover, for the general case $m_A \lesssim M_{\text{SUSY}}$, we provide analytical formulae (including two-loop leading-log corrections) for all the masses and couplings in the Higgs sector. For $M_{\text{SUSY}} \lesssim 1.5$ TeV and arbitrary values of m_A , $\tan\beta$ and the stop mixing parameters, they reproduce the numerical renormalization-group improved leading-log result for the Higgs masses with an error of less than 3 GeV. For the Higgs couplings, our analytical formulae reproduce the numerical results equally well. Comparison with other methods is also performed.

CERN-TH/95-45

March 1995

*Work supported in part by the European Union (contract CHRX-CT92-0004) and CICYT of Spain (contract AEN94-0928).

[†]On leave of absence from Instituto de Estructura de la Materia, CSIC, Serrano 123, 28006-Madrid, Spain.

1 Introduction

The most appealing extension of the Standard Model (SM) is the Minimal Supersymmetric Standard Model (MSSM), which can provide a technical explanation for the hierarchy stability from M_{Pl} to the electroweak scale. From the experimental point of view, the MSSM is also attractive and presents clear and distinct signatures. In particular, its Higgs sector predicts the existence of a light CP-even state with a mass which cannot exceed a value of ~ 150 GeV, unlike the case of the SM Higgs whose mass can reach much larger values (~ 1 TeV). The precise bounds on the mass spectrum of the MSSM Higgs bosons strongly depend on the value of the top-quark mass M_t [1, 2].

In view of Higgs searches at future colliders, and of the fact that the top-quark mass is being measured at the Tevatron [3, 4], it is of the highest interest to provide determinations as precise as possible of the radiatively corrected Higgs mass spectrum and Higgs couplings and, in particular, to find accurate upper bounds on the mass of the lightest Higgs boson. To this end one can assume that $M_W \ll M_{\text{SUSY}} \lesssim \mathcal{O}(\text{few})$ TeV, where M_{SUSY} is the characteristic supersymmetry particle mass scale and its upper limit is determined by naturalness arguments. In this case the upper bound on the lightest Higgs mass is reached when the mass of the CP-odd Higgs, m_A , is of the order of M_{SUSY} , and the theory below M_{SUSY} is the SM with threshold effects at M_{SUSY} . For values of $m_A < M_{\text{SUSY}}$ the theory below M_{SUSY} is the two-Higgs doublet model, and then, two CP-even and one CP-odd neutral Higgs bosons, and two charged Higgs bosons appear in the physical spectrum below M_{SUSY} .

It is the aim of this letter to explore the whole range $m_A \lesssim M_{\text{SUSY}}$ and provide an accurate numerical evaluation as well as analytical formulae for the whole Higgs mass spectrum and Higgs couplings of the MSSM. We shall also compute the range of validity of our approximations, as well as make comparison with other methods currently used in the literature.

2 The case $m_A \sim M_{\text{SUSY}}$

This case is well described, as we mentioned above, by the SM with the quartic coupling

$$\lambda = \frac{1}{4}(g_2^2 + g_1^2) \cos^2 2\beta \quad (1)$$

at M_{SUSY} , and one-loop threshold contributions at that scale

$$\Delta\lambda = \frac{3}{16\pi^2} (h_t^{\text{SM}})^4 \tilde{X}_t. \quad (2)$$

In the above, g_2 and g_1 are the $SU(2) \times U(1)_Y$ gauge couplings, $\tan \beta = v_2/v_1$ is the ratio of the vacuum expectation values of the neutral components of the two supersymmetric Higgs bosons, h_t^{SM} is the SM top-quark Yukawa coupling and \tilde{X}_t is the stop mixing parameter ¹:

$$\tilde{X}_t = \frac{2\tilde{A}_t^2}{M_{\text{SUSY}}^2} \left(1 - \frac{\tilde{A}_t^2}{12M_{\text{SUSY}}^2} \right)$$

¹In this section we are neglecting the sbottom mixing parameter.

$$\tilde{A}_t = A_t - \mu \cot \beta. \quad (3)$$

The supersymmetric scale M_{SUSY} is taken as the squared root of the arithmetical average of the diagonal entries in the squared squark mass matrix and, for simplicity, we assume that all supersymmetric particle masses are of order M_{SUSY} . A more detailed discussion about the definition of M_{SUSY} and the possible effect of light sparticles will be given in sections 4 and 5.

The Higgs boson mass was first determined by renormalization-group resummation of all-loop leading-log (LL) corrections [5, 6, 7, 8]. Some next-to-leading-log (NTLL) corrections were further introduced [9, 10] and finally a complete NTLL analysis was performed in Refs. [11, 12].

In Ref. [12] physical pole masses for the top-quark and Higgs-boson were used and the dependence with respect to the renormalization-group scale in the NTLL approximation was explicitly analysed. One of the main issues in [12] was the comparison between the LL and NTLL approximations. As expected, the LL approximation shows strong scale dependence, while the NTLL is almost scale independent. This implies not only that the choice of the renormalization-group scale is irrelevant when working in the NTLL approximation, but also that a judicious choice of the renormalization scale in the LL approximation can yield very accurate results. It turns out that, independently of the value of the stop mixing parameter, the scale where both results coincide is very close to the pole top-quark mass M_t (see e.g. Fig. 8 of Ref. [12]).

This result can also be understood from Ref. [13] where the physical Higgs mass is related to the quartic coupling in the $\overline{\text{MS}}$ scheme, $\lambda(t)$. One can write

$$M_h^2 = m_h^2(t)(1 - \delta - \Delta r) \quad (4)$$

where

$$m_h^2(t) = 2\lambda(t)v^2 \quad (5)$$

is the running Higgs mass, and $v = 174.1$ GeV. From [13, 14], and neglecting scalar and electroweak gauge couplings, we can write

$$\begin{aligned} \delta + \Delta r &= \frac{3}{16\pi^2} (h_t^{\text{SM}})^2 \left(2 - 4 \frac{M_t^2}{M_h^2} \right) \log \frac{Q^2}{M_t^2} + \varepsilon \\ \varepsilon &= -\frac{3}{16\pi^2} (h_t^{\text{SM}})^2 \left[Z \left(\frac{M_t^2}{M_h^2} \right) - 2 \right] \left(1 - 4 \frac{M_t^2}{M_h^2} \right) \end{aligned} \quad (6)$$

where Q is the renormalization scale and the function $Z(x)$ is given, for $x > 1/4$, by

$$Z(x) = 2\sqrt{4x - 1} \tan^{-1}(1/\sqrt{4x - 1}). \quad (7)$$

We can see from (6) that choosing $Q = M_t$, the difference between the pole mass and the running mass is determined by ε ($\varepsilon \leq 1.7\%$ for $M_h \geq 60$ GeV and $M_t \leq 200$ GeV). For instance for $M_h = 90$ GeV and $M_t = 180$ GeV, then $\varepsilon = 1.3\%$. Other values of Q (e.g. $Q = M_Z$ as can be usually found in the literature [15]) can provide much larger corrections, depending on the values of M_h and M_t , unless an appropriate decoupling of the top-quark effects below the top-quark mass scale is performed.

For the Higgs mass, we shall therefore adopt the value provided by (5) with $Q = M_t$ and work in the LL approximation as suggested by (6). We compare, in Fig. 1, the all-loop RG improved NTLL [12] (solid) and LL (dashed) lines for $M_{\text{SUSY}} = 1$ TeV. We consider the case of zero mixing, $\tilde{X}_t = 0$, and the case $\tilde{X}_t = 6$, which maximizes the lightest CP-even Higgs mass, large values of $\tan\beta$ ($\tan\beta = 15$) and small values of $\tan\beta$ [the infrared (IR) fixed point solution with $\sin\beta \sim (200 \text{ GeV})/M_t$]. The RG improved LL approximation involves the one-loop RG running of the couplings, the one-loop threshold effects $\Delta\lambda$, Eq. (2), from the decoupling of the supersymmetric particles at M_{SUSY} , and the computation of the Higgs masses at the scale $Q = M_t$. Moreover, in both approximations the pole top-quark mass M_t was computed from the on-shell running mass m_t through the corresponding one-loop QCD correction factor

$$m_t = \frac{M_t}{1 + \frac{4}{3\pi}\alpha_3(M_t)}. \quad (8)$$

We see that, for all values of the top-quark mass, $\tan\beta$ and the stop mixing parameter, the solid and dashed curves agree with each other with an accuracy better than 2 GeV.

We have also worked out an analytical approximation to the numerical all-loop renormalization-group improved LL result, including two-loop leading-log effects. It is given by

$$\begin{aligned} m_h^2 &= M_Z^2 \cos^2 2\beta \left(1 - \frac{3}{8\pi^2} \frac{m_t^2}{v^2} t \right) \\ &+ \frac{3}{4\pi^2} \frac{m_t^4}{v^2} \left[\frac{1}{2} \tilde{X}_t + t + \frac{1}{16\pi^2} \left(\frac{3}{2} \frac{m_t^2}{v^2} - 32\pi\alpha_3 \right) (\tilde{X}_t t + t^2) \right] \end{aligned} \quad (9)$$

where the angle β is defined here at the scale M_{SUSY} ,

$$t = \log \frac{M_{\text{SUSY}}^2}{M_t^2}, \quad (10)$$

and

$$\alpha_3(M_t) = \frac{\alpha_3(M_Z)}{1 + \frac{b_3}{4\pi}\alpha_3(M_Z) \log(M_t^2/M_Z^2)}, \quad (11)$$

where $b_3 = 11 - 2N_f/3$ is the one-loop QCD beta function and N_f is the number of quark flavours, which is equal to 5 at scales below M_t . Notice that Eq. (9) includes the leading D -term correction $\mathcal{O}(M_Z^2 m_t^2)$. As was pointed out in Ref. [16], this contribution cannot be neglected, since, for the experimental M_t range, it can account for a (negative) shift as large as ~ 5 GeV. Formula (9) is also plotted in Fig. 1 (dotted lines), for the same values of the supersymmetric parameters as before. We can see that the analytical approximation reproduces the numerical results within an error of less than 2 GeV in all cases.

Finally, in Fig. 2 we have plotted the Higgs mass, in the three different approximations, for $M_t = 175$ GeV, as a function of M_{SUSY} . As expected the NTLL (solid) and LL (dashed) curves coincide within less than 2 GeV difference. The analytical approximation also remains within this level of accuracy if $M_{\text{SUSY}} \lesssim 1.5$ TeV. Hence,

it follows that for higher values of M_{SUSY} , agreement with numerical results would demand the addition of $\mathcal{O}(t^3)$ terms (three-loop leading-log), but for the theoretically preferred values of the supersymmetry breaking scale, $M_{\text{SUSY}} \lesssim 1$ TeV, the analytical formula provides excellent results. For values of $M_{\text{SUSY}} \leq 500$ GeV, the maximal value of the mixing parameter \tilde{X}_t is restricted (see discussion in section 4).

3 The case $m_A \lesssim M_{\text{SUSY}}$

In the more general case, $m_A \lesssim M_{\text{SUSY}}$, the effective theory below the scale M_{SUSY} [8] is a two-Higgs doublet model where the tree level quartic couplings can be written in terms of dimensionless parameters λ_i , $i = 1, \dots, 7$, whose tree level values are functions of the gauge couplings, and with one-loop threshold corrections $\Delta\lambda_i$, $i = 1, \dots, 7$, expressed as functions of the supersymmetric Higgs mass μ and the soft supersymmetry breaking parameters A_t , A_b and m_A . We are using the conventions of Ref. [8]. Motivated by the previous agreement among the NTLL and LL approximations and the analytical formulae, we can safely extrapolate the analytical approach, to obtain the two-loop results for the Higgs spectrum within the MSSM.

The CP-even light and heavy Higgs masses and the charged Higgs mass are given as functions of $\tan\beta$, M_{SUSY} , A_t , A_b , μ , the CP-odd Higgs mass m_A and the physical top-quark mass M_t related to the on-shell running mass m_t through Eq. (8). We present below the masses and mixing angle of the Higgs sector as functions of the parameters λ_i , for which we have derived the corresponding analytical formulae and which are the equivalent in the two-Higgs doublet model of the analytical approximation (9) for the case of the SM. For completeness, we include the bottom Yukawa coupling effects, which may become large for values of $\tan\beta \simeq m_t/m_b$, where m_b is the running bottom mass at the scale M_t .

The two CP-even and the charged Higgs masses read

$$m_{h(H)}^2 = \frac{\text{Tr}M^2 \mp \sqrt{(\text{Tr}M^2)^2 - 4 \det M^2}}{2} \quad (12)$$

$$m_{H^\pm}^2 = m_A^2 + (\lambda_5 - \lambda_4)v^2, \quad (13)$$

where

$$\text{Tr}M^2 = M_{11}^2 + M_{22}^2 ; \quad \det M^2 = M_{11}^2 M_{22}^2 - (M_{12}^2)^2, \quad (14)$$

with

$$\begin{aligned} M_{12}^2 &= 2v^2[\sin\beta \cos\beta(\lambda_3 + \lambda_4) + \lambda_6 \cos^2\beta + \lambda_7 \sin^2\beta] - m_A^2 \sin\beta \cos\beta \\ M_{11}^2 &= 2v^2[\lambda_1 \cos^2\beta + 2\lambda_6 \cos\beta \sin\beta + \lambda_5 \sin^2\beta] + m_A^2 \sin^2\beta \\ M_{22}^2 &= 2v^2[\lambda_2 \sin^2\beta + 2\lambda_7 \cos\beta \sin\beta + \lambda_5 \cos^2\beta] + m_A^2 \cos^2\beta. \end{aligned} \quad (15)$$

The mixing angle α is equally determined by

$$\sin 2\alpha = \frac{2M_{12}^2}{\sqrt{(\text{Tr}M^2)^2 - 4 \det M^2}} \quad (16)$$

$$\cos 2\alpha = \frac{M_{11}^2 - M_{22}^2}{\sqrt{(\text{Tr} M^2)^2 - 4 \det M^2}} \quad (17)$$

The above quartic couplings are given by

$$\begin{aligned} \lambda_1 &= \frac{g_1^2 + g_2^2}{4} \left(1 - \frac{3}{8\pi^2} h_b^2 t \right) \\ &+ \frac{3}{8\pi^2} h_b^4 \left[t + \frac{X_b}{2} + \frac{1}{16\pi^2} \left(\frac{3}{2} h_b^2 + \frac{1}{2} h_t^2 - 8 g_3^2 \right) (X_b t + t^2) \right] \\ &- \frac{3}{96\pi^2} h_t^4 \frac{\mu^4}{M_{\text{SUSY}}^4} \left[1 + \frac{1}{16\pi^2} (9 h_t^2 - 5 h_b^2 - 16 g_3^2) t \right] \end{aligned} \quad (18)$$

$$\begin{aligned} \lambda_2 &= \frac{g_1^2 + g_2^2}{4} \left(1 - \frac{3}{8\pi^2} h_t^2 t \right) \\ &+ \frac{3}{8\pi^2} h_t^4 \left[t + \frac{X_t}{2} + \frac{1}{16\pi^2} \left(\frac{3}{2} h_t^2 + \frac{h_b^2}{2} - 8 g_3^2 \right) (X_t t + t^2) \right] \\ &- \frac{3}{96\pi^2} h_b^4 \frac{\mu^4}{M_{\text{SUSY}}^4} \left[1 + \frac{1}{16\pi^2} (9 h_b^2 - 5 h_t^2 - 16 g_3^2) t \right] \end{aligned} \quad (19)$$

$$\begin{aligned} \lambda_3 &= \frac{g_2^2 - g_1^2}{4} \left(1 - \frac{3}{16\pi^2} (h_t^2 + h_b^2) t \right) \\ &+ \frac{6}{16\pi^2} h_t^2 h_b^2 \left[t + \frac{A_{tb}}{2} + \frac{1}{16\pi^2} (h_t^2 + h_b^2 - 8 g_3^2) (A_{tb} t + t^2) \right] \\ &+ \frac{3}{96\pi^2} h_t^4 \left[\frac{3\mu^2}{M_{\text{SUSY}}^2} - \frac{\mu^2 A_t^2}{M_{\text{SUSY}}^4} \right] \left[1 + \frac{1}{16\pi^2} (6 h_t^2 - 2 h_b^2 - 16 g_3^2) t \right] \\ &+ \frac{3}{96\pi^2} h_b^4 \left[\frac{3\mu^2}{M_{\text{SUSY}}^2} - \frac{\mu^2 A_b^2}{M_{\text{SUSY}}^4} \right] \left[1 + \frac{1}{16\pi^2} (6 h_b^2 - 2 h_t^2 - 16 g_3^2) t \right] \end{aligned} \quad (20)$$

$$\begin{aligned} \lambda_4 &= -\frac{g_2^2}{2} \left(1 - \frac{3}{16\pi^2} (h_t^2 + h_b^2) t \right) \\ &- \frac{6}{16\pi^2} h_t^2 h_b^2 \left[t + \frac{A_{tb}}{2} + \frac{1}{16\pi^2} (h_t^2 + h_b^2 - 8 g_3^2) (A_{tb} t + t^2) \right] \\ &+ \frac{3}{96\pi^2} h_t^4 \left[\frac{3\mu^2}{M_{\text{SUSY}}^2} - \frac{\mu^2 A_t^2}{M_{\text{SUSY}}^4} \right] \left[1 + \frac{1}{16\pi^2} (6 h_t^2 - 2 h_b^2 - 16 g_3^2) t \right] \\ &+ \frac{3}{96\pi^2} h_b^4 \left[\frac{3\mu^2}{M_{\text{SUSY}}^2} - \frac{\mu^2 A_b^2}{M_{\text{SUSY}}^4} \right] \left[1 + \frac{1}{16\pi^2} (6 h_b^2 - 2 h_t^2 - 16 g_3^2) t \right] \end{aligned} \quad (21)$$

$$\begin{aligned} \lambda_5 &= -\frac{3}{96\pi^2} h_t^4 \frac{\mu^2 A_t^2}{M_{\text{SUSY}}^4} \left[1 - \frac{1}{16\pi^2} (2 h_b^2 - 6 h_t^2 + 16 g_3^2) t \right] \\ &- \frac{3}{96\pi^2} h_b^4 \frac{\mu^2 A_b^2}{M_{\text{SUSY}}^4} \left[1 - \frac{1}{16\pi^2} (2 h_t^2 - 6 h_b^2 + 16 g_3^2) t \right] \end{aligned} \quad (22)$$

$$\begin{aligned}\lambda_6 &= \frac{3}{96\pi^2} h_t^4 \frac{\mu^3 A_t}{M_{\text{SUSY}}^4} \left[1 - \frac{1}{16\pi^2} \left(\frac{7}{2} h_b^2 - \frac{15}{2} h_t^2 + 16g_3^2 \right) t \right] \\ &+ \frac{3}{96\pi^2} h_b^4 \frac{\mu}{M_{\text{SUSY}}} \left(\frac{A_b^3}{M_{\text{SUSY}}^3} - \frac{6A_b}{M_{\text{SUSY}}} \right) \left[1 - \frac{1}{16\pi^2} \left(\frac{1}{2} h_t^2 - \frac{9}{2} h_b^2 + 16g_3^2 \right) t \right]\end{aligned}\quad (23)$$

$$\begin{aligned}\lambda_7 &= \frac{3}{96\pi^2} h_b^4 \frac{\mu^3 A_b}{M_{\text{SUSY}}^4} \left[1 - \frac{1}{16\pi^2} \left(\frac{7}{2} h_t^2 - \frac{15}{2} h_b^2 + 16g_3^2 \right) t \right] \\ &+ \frac{3}{96\pi^2} h_t^4 \frac{\mu}{M_{\text{SUSY}}} \left(\frac{A_t^3}{M_{\text{SUSY}}^3} - \frac{6A_t}{M_{\text{SUSY}}} \right) \left[1 - \frac{1}{16\pi^2} \left(\frac{1}{2} h_b^2 - \frac{9}{2} h_t^2 + 16g_3^2 \right) t \right],\end{aligned}\quad (24)$$

which contain the same kind of corrections as Eq. (9), including the leading D -term contributions, and where we have defined,

$$\begin{aligned}X_t &= \frac{2A_t^2}{M_{\text{SUSY}}^2} \left(1 - \frac{A_t^2}{12M_{\text{SUSY}}^2} \right) \\ X_b &= \frac{2A_b^2}{M_{\text{SUSY}}^2} \left(1 - \frac{A_b^2}{12M_{\text{SUSY}}^2} \right) \\ A_{tb} &= \frac{1}{6} \left[-\frac{6\mu^2}{M_{\text{SUSY}}^2} - \frac{(\mu^2 - A_b A_t)^2}{M_{\text{SUSY}}^4} + \frac{3(A_t + A_b)^2}{M_{\text{SUSY}}^2} \right].\end{aligned}\quad (25)$$

All quantities in the approximate formulae are defined at the scale M_t . In particular $\alpha_3(M_t)$ is given in Eq. (11), and

$$\begin{aligned}h_t &= m_t(M_t)/(v \sin \beta) \\ h_b &= m_b(M_t)/(v \cos \beta)\end{aligned}\quad (26)$$

are the top and bottom Yukawa couplings in the two-Higgs doublet model.

For $m_A \leq M_t$, $\tan \beta$ is fixed at the scale m_A , while for $m_A \geq M_t$, $\tan \beta$ is given by [16]

$$\tan \beta(M_t) = \tan \beta(m_A) \left[1 + \frac{3}{32\pi^2} (h_t^2 - h_b^2) \log \frac{m_A^2}{M_t^2} \right]. \quad (27)$$

For the case in which the CP-odd Higgs mass m_A is lower than M_{SUSY} , but still larger than the top-quark mass scale, we decouple, in the numerical computations, the heavy Higgs doublet and define an effective quartic coupling for the light Higgs, which is related to the running Higgs mass at the scale m_A through

$$\lambda(m_A) = \frac{m_h(m_A)}{2v^2}. \quad (28)$$

The low energy value of the quartic coupling is then obtained by running the SM renormalization-group equations from the scale m_A down to the scale M_t . In the analytical approximation, for simplicity we ignore the effect of decoupling the heavy

Higgs doublet at an intermediate scale. We partially compensate the effect of this approximation by relating the value of $\tan\beta$ at the scale M_t with its corresponding value at the scale m_A through its renormalization-group running, Eq. (27).

In Figs. 3, 4 and 5 we plot m_h , m_H and m_H^\pm , respectively, as functions of m_A , for $M_t = 175$ GeV and the four cases corresponding to $\tan\beta = 15$ and $\tan\beta \simeq 1.6$ (which is the lowest possible value of $\tan\beta$ for this M_t and corresponds to the IR fixed point solution) and for large and zero mixing. Solid curves correspond to the numerical renormalization-group improved LL approximation and dashed curves to the analytical approximation depicted in the previous formulae. For the charged Higgs mass, we have also plotted the case $\mu = 2M_{\text{SUSY}}$ and $\tan\beta = 15$, since, unless large values of $\tan\beta \simeq m_t/m_b$ are considered, its radiative corrections depend on μ but not on A_t or A_b (see Eqs. (21) and (22)). We can observe that, in all cases, the agreement between the Higgs masses in the numerical renormalization-group improved calculation and the analytical approximation is, either of the order of, or better than, 3 GeV.

Vertex	Coupling
$\{h, H\}W_\mu W_\nu$	$ig_2 M_W g_{\mu\nu} \{\sin(\beta - \alpha), \cos(\alpha + \beta)\}$
$\{h, H\}Z_\mu Z_\nu$	$ig_2 \frac{M_W}{\cos^2 \theta_W} g_{\mu\nu} \{\sin(\beta - \alpha), \cos(\alpha + \beta)\}$
$\{h, H, A\}u\bar{u}$	$-\frac{i}{2} \left(\frac{m_u}{M_W} \right) \frac{g_2}{\sin \beta} \{\cos \alpha, \sin \alpha, -i\gamma_5 \cos \beta\}$
$\{h, H, A\}d\bar{d}$	$-\frac{i}{2} \left(\frac{m_d}{M_W} \right) \frac{g_2}{\cos \beta} \{-\sin \alpha, \cos \alpha, -i\gamma_5 \sin \beta\}$
$\{h, H\}AZ_\mu$	$-\frac{e(p+k)_\mu}{2 \cos \theta_W \sin \theta_W} \{\cos(\beta - \alpha), -\sin(\beta - \alpha)\}$

Notice that the knowledge of the radiatively corrected quartic couplings λ_i , $i = 1, \dots, 7$, and hence of the corresponding value of the Higgs mixing angle α , permits the evaluation of all radiatively corrected Higgs couplings. For instance some important Yukawa and gauge Higgs couplings [17] are listed in the table above, where p_μ (k_μ) is the incoming (outcoming) CP-odd (CP-even) Higgs momentum. Furthermore, the trilinear Higgs couplings can be explicitly written as functions of λ_i , $i = 1, \dots, 7$, α and β [8, 18]. To check the goodness of our analytical approximation on the different couplings we plot in Fig. 6, for the same four cases as in Figs. 3–5, $\cos \alpha$ as a function of m_A , for $M_t = 175$ GeV. As can be seen from Fig. 6, we find excellent agreement between the values obtained with the numerical and analytical approximations.

4 On the expansion variables

In this section we shall comment on the definition of M_{SUSY} . As we mentioned above, the scale M_{SUSY} , appearing in the quartic coupling expressions, should be associated with a characteristic squark mass scale. The renormalization group analysis considered in this work is based on the assumption of a single step decoupling of the squark fields, which is valid only if the mass splitting among the squark mass eigenstates is small. More quantitatively, the validity of our expansion requires,

$$\frac{m_{\tilde{t}_1}^2 - m_{\tilde{t}_2}^2}{m_{\tilde{t}_1}^2 + m_{\tilde{t}_2}^2} \lesssim 0.5, \quad (29)$$

where $m_{\tilde{t}_1}^2$ and $m_{\tilde{t}_2}^2$ are the stop squared mass eigenvalues. This restriction also applies to all existing Higgs mass analyses at the next-to leading order [10–12]. Observe that Eq. (29) automatically ensures the absence of tachyons in the stop sector. Furthermore, under the validity of Eq. (29), the scale M_{SUSY}^2 may be safely defined as the arithmetic average of the stop squared mass eigenvalues,

$$M_{\text{SUSY}}^2 = \frac{m_{\tilde{t}_1}^2 + m_{\tilde{t}_2}^2}{2}. \quad (30)$$

Observe that our work, as well as all other RG Higgs mass analyses performed in the literature, also relies on an expansion of the effective Higgs potential up to operators of dimension four. The contribution of higher dimensional operators may be safely neglected only if $2|M_t A_t| < M_{\text{SUSY}}^2$ and $2|M_t \mu| < M_{\text{SUSY}}^2$.

Strictly speaking, the operator expansion was performed in the symmetric phase, where the squared of the energy scale at which the stops decouple is not the average of the stop squared masses, M_{SUSY} , but the average of the stop soft supersymmetry breaking squared mass parameters, $m^2 \equiv (m_Q^2 + m_U^2)/2$. Higher dimensional operators in the symmetric phase can only be neglected if $M_{\text{SUSY}}^2 \gg M_t^2$. In this range of parameters, the distinction between M_{SUSY} and the real decoupling scale has no impact on our approximations. In general, our expressions give a reliable approximation to the Higgs masses whenever the above restriction on the stop mixing parameter, Eq. (29), holds, and $M_{\text{SUSY}} \gtrsim 2M_t$. Moreover, for the large $\tan\beta$ case, for which the bottom-Yukawa contribution becomes relevant, we have assumed that the sbottom masses are of order of the stop ones and that similar bounds on their mixing mass parameters are fulfilled.

Physically it is clear that, in the region where higher order operators are unsuppressed, $M_{\text{SUSY}} \lesssim 2M_t$, the leading logarithm expansion of the Higgs masses should contain powers of $\log(M_{\text{SUSY}}^2/M_t^2)$ rather than $\log(m^2/M_t^2)$. This should be the case, since, in the supersymmetric limit for the top/stop sector, $M_{\text{SUSY}} = M_t$, and zero mixing, one should recover the tree level values for the Higgs masses. One may ask how accurately our analytical expressions may determine the Higgs masses for values of $M_{\text{SUSY}} \lesssim 2M_t$, for which, strictly speaking, one is beyond the limits of the present expansion. In fact, in order to check the reliability of our approximation for the case in which light stops, with masses of the order of the top mass, are present, an alternative computation, valid in that regime, should be used. The expressions for the

CP-even Higgs mass matrix elements computed in Ref. [2], and based on the one-loop effective potential in the MSSM (keeping the leading supersymmetric corrections from the stop/sbottom sectors) can be useful for the comparison. Observe that the MSSM effective potential is valid only at scales of the order of, or larger than, the characteristic stop supersymmetry breaking terms. One cannot consider the MSSM effective potential at scales below the squark masses since, at those scales, the squarks are already decoupled, possibly leaving threshold corrections to match the effective potential beyond and below the supersymmetric threshold.

Once recognized that the MSSM effective potential is valid at the scale defined by the squark masses, one can try to *improve* its performance by means of its RG improvement [19]. Were the RG improved effective potential exactly scale independent, one could minimize it at any scale (e.g. at M_{SUSY}), defining all the running parameters on which the effective potential depends also at that scale, and rewrite them, in turn, as functions of the corresponding parameters defined at the scale M_t . Then, taking advantage of the scale independence of the effective potential one could run the Higgs masses from the high scale to M_t using the anomalous dimensions of the Higgs fields. However, the RG improved one-loop effective potential is not exactly scale independent (even after including all LL and NTLL corrections) and hence, when minimizing it at M_{SUSY} (see e.g. Figs. 1 and 3 in Ref. [12]) one is implicitly including an error in the lightest CP-even Higgs mass determination. This error is very small for values of M_{SUSY} of the order of the weak scale, but becomes significant for larger scales (e.g. $M_{\text{SUSY}} \gtrsim 500$ GeV).

We therefore consider the RG improved MSSM effective potential, which is minimized at the scale M_{SUSY} , at which we determine the neutral Higgs boson squared mass matrix. All the parameters in the mass matrix are running parameters, defined at the scale M_{SUSY} (including the vacuum expectation values v_1 and v_2). They are related to parameters defined at the scale M_t by the corresponding evolution with the β - and γ -functions, that we compute to one-loop LL (i.e. first order in the expansion parameter $\log(M_{\text{SUSY}}^2/M_t^2)$) and keeping only the Yukawa and strong gauge couplings, as in our analytical expressions of sections 2 and 3. We then evolve the squared mass matrix, with the corresponding anomalous dimension matrix, from M_{SUSY} to M_t . In Fig. 7 we plot the lightest CP-even Higgs mass obtained from our analytical expressions (solid lines) and that obtained from the RG improved effective potential of the MSSM (dashed lines), for a pole top-quark mass $M_t = 175$ GeV, vanishing mixing $A_t = \mu = 0$, $m_A = M_{\text{SUSY}}$ (to simplify the comparison), and large ($\tan\beta = 15$) and small (IR) values of $\tan\beta$. We can see that the agreement between the Higgs masses obtained by using our analytical expressions and the RG improved MSSM effective potential is very good for all values of $M_{\text{SUSY}} \lesssim 500$ GeV, and in particular for $M_{\text{SUSY}} \lesssim 2M_t$, for which the latter should give a reliable description. Hence, we see that, independently of the value of $\tan\beta$, our analytical expressions give a very good approximation to the Higgs mass values, in the case of no left-right stop mixing, even in the regime $M_{\text{SUSY}} \lesssim 2M_t$. For the case of stop mixing considered in Fig. 8, observe that, independently of the value of $\tan\beta$, the results are also in very good agreement for values of $M_{\text{SUSY}} \lesssim 500$ GeV. Similar conclusions may be obtained for any value of the stop mixing parameter.

Observe that, in order to compute pole Higgs masses, Higgs vacuum polarization

contributions should be added to our computation. As we discussed in section 2, by fixing the renormalization scale to the pole top-quark mass, we make the top-dependent vacuum polarization contributions small. The stop-dependent contributions are renormalization-scale independent. For light stops, these contributions are opposite in sign to the top leading ones and of the same order of magnitude; they become very small if the stops are heavy. In general, for our choice of the renormalization scale, the vacuum polarization contributions are small, and would only be required in a computation of Higgs masses going beyond the approximation presented in the present work.

Summarizing, even for stop masses of order of the top mass, our analytical expressions give a very good approximation to the Higgs mass value. Observe that, since we have applied one step decoupling on the stops, the constraint on the stop mass splitting, Eq. (29), should always be held. Finally, in Figs. 7 and 8 we also plot, for comparison, the values obtained from the MSSM effective potential while ignoring the RG improvement, and evaluating all running masses and couplings directly at the scale M_t (dotted lines). In particular, we use, for the top mass, the running value $m_t(M_t)$. This approximation overestimates the Higgs mass for basically all values of M_{SUSY} .

5 Conclusions

In this work we present a one-loop improved renormalization-group analysis of the lightest CP-even Higgs mass, which, for the case $m_A \sim M_{\text{SUSY}}$, reproduces the existing two-loop renormalization-group improved effective potential results within an error of less than 2 GeV. For the general case $m_A \lesssim M_{\text{SUSY}}$, we provide an analytical approximation (including two-loop leading-log corrections) for the effective quartic couplings, which determines the Higgs mass spectrum within an error of less than 3 GeV with respect to the values obtained using the improved one loop RG approximation. Our formulae are also useful to write radiatively corrected expressions for the Higgs couplings, which are of interest in computing physical processes.

Our analysis takes into account the dominant top and bottom quark Yukawa (as well as strong gauge) coupling effects, by assuming a characteristic supersymmetric scale, M_{SUSY} , and including squark mixing effects. In some realistic scenarios the chargino and neutralino masses may become much smaller than the characteristic squark mass scale. Light charginos and neutralinos have a small and negative effect on the lightest CP-even Higgs mass, of order 2–3 GeV [2, 20], which may be added to our analytical approximation at the one-loop order.

Our approximation relies on a one step decoupling of all supersymmetric particles and, in particular, on the stop mixing parameter requirements discussed in section 4. A computation of the Higgs masses and couplings going beyond the approximation presented in this work, would demand the derivation of the full two-loop RG improvement of the one-loop effective potential, and polarization corrections to running Higgs masses, including the squark and heavy Higgs contributions, the analogous to what has been done for the case of large squark and CP-odd Higgs masses in Ref. [12]. We expect to come back to this subject elsewhere.

Acknowledgements

The work of J.R.E. is supported by the Alexander-von-Humboldt Stiftung. The work of C.W. and M.C. is partially supported by the Worldlab. We wish to thank J.-F. Grivaz, H.E. Haber, R. Hempfling, A. Hoang and F. Zwirner for useful discussions and comments.

References

- [1] Y. Okada, M. Yamaguchi and T. Yanagida, *Prog. Theor. Phys.* **85** (1991) 1; H.E. Haber and R. Hempfling, *Phys. Rev. Lett.* **66** (1991) 1815
- [2] J. Ellis, G. Ridolfi and F. Zwirner, *Phys. Lett.* **B257** (1991) 83; *Phys. Lett.* **B262** (1991) 477; A. Brignole, J. Ellis, G. Ridolfi and F. Zwirner, *Phys. Lett.* **B271** (1991) 123
- [3] F. Abe et al., CDF Collaboration, *Phys. Rev.* **D50** (1994) 2966; *Phys. Rev. Lett.* **73** (1994) 225; preprint FERMILAB-PUB-95/022-E (2 March 1995)
- [4] S. Abachi et al., D0 Collaboration, *Phys. Rev. Lett.* **72** (1994) 2138; preprint FERMILAB-PUB-354/E, to appear in *Phys. Rev. Lett.* **74** (1995) 2422; preprint FERMILAB-PUB-95/028-E (3 March 1995)
- [5] R. Barbieri, M. Frigeni and F. Caravaglios, *Phys. Lett.* **B258** (1991) 167
Y. Okada, M. Yamaguchi and T. Yanagida, *Phys. Lett.* **B262** (1991) 54
- [6] M. Carena, K. Sasaki and C.E.M. Wagner, *Nucl. Phys.* **B381** (1992) 66
- [7] P. Chankowski, S. Pokorski and J. Rosiek, *Phys. Lett.* **B274** (1992) 191
- [8] H.E. Haber and R. Hempfling, *Phys. Rev.* **D48** (1993) 4280
- [9] J.R. Espinosa and M. Quirós, *Phys. Lett.* **B266** (1991) 389
- [10] R. Hempfling and A.H. Hoang, *Phys. Lett.* **B331** (1994) 99
- [11] J. Kodaira, Y. Yasui and K. Sasaki, *Phys. Rev.* **D50** (1994) 7035
- [12] J.A. Casas, J.R. Espinosa, M. Quirós and A. Riotto, *Nucl. Phys.* **B436** (1995) 3
- [13] A. Sirlin and R. Zucchini, *Nucl. Phys.* **B266** (1986) 389
- [14] W.J. Marciano and A. Sirlin, *Phys. Rev.* **D22** (1980) 2695
- [15] P. Langacker and N. Polonsky, *Phys. Rev.* **D50** (1994) 2199
- [16] A. Brignole, *Phys. Lett.* **B281** (1992) 284
- [17] See, e.g., J. Rosiek, *Phys. Rev.* **D41** (1991) 3464
- [18] H.E. Haber, R. Hempfling and Y. Nir, *Phys. Rev.* **D46** (1992) 3015
- [19] C. Ford, D.R.T. Jones, P.W. Stevenson and M.B. Einhorn, *Nucl. Phys.* **B395** (1993) 17
- [20] S.P. Li and M. Sher, *Phys. Lett.* **B140** (1984) 339;
P.H. Chankowski, S. Pokorski and J. Rosiek, *Phys. Lett.* **B274** (1992) 191;
Nucl. Phys. **B243** (1994) 437;
A. Dabelstein, Univ. Karlsruhe preprint, hep-ph/9409375

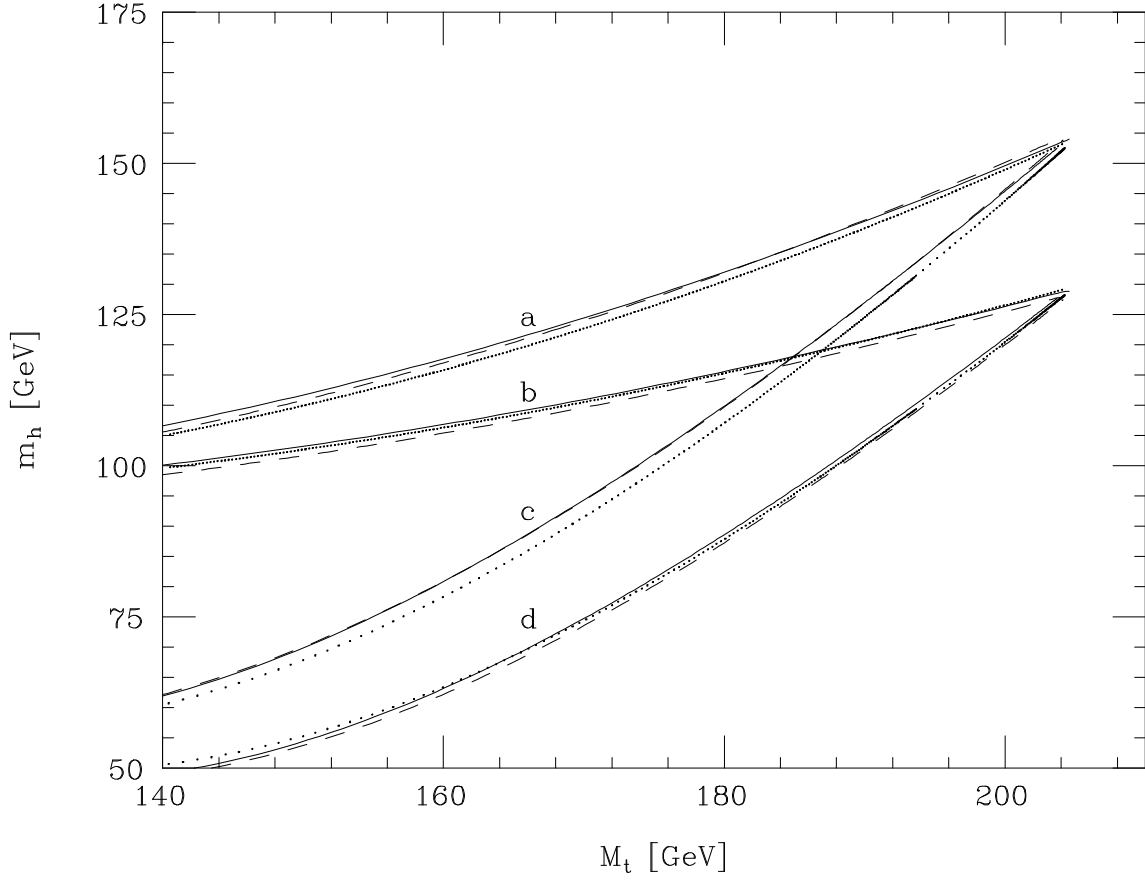


Figure 1: The lightest CP-even Higgs mass as a function of the physical top-quark mass, for $M_{\text{SUSY}} = 1$ TeV, evaluated in the limit of large CP-odd Higgs mass, as obtained from the two-loop renormalization-group improved effective potential (solid lines), the one-loop improved RG evolution (dashed lines) and the analytical formulae, Eq. (9) (dotted lines). The four sets of lines correspond to: **a**) $\tan \beta = 15$ with maximal squark mixing, $\tilde{X}_t = 6$; **b**) $\tan \beta = 15$ with zero mixing, $\tilde{X}_t = 0$; **c**) the minimal value of $\tan \beta$ allowed by perturbativity constraints for the given value of M_t (IR fixed point), with $\tilde{X}_t = 6$; and, **d**) $\tan \beta$ the same as in (c) with zero mixing.

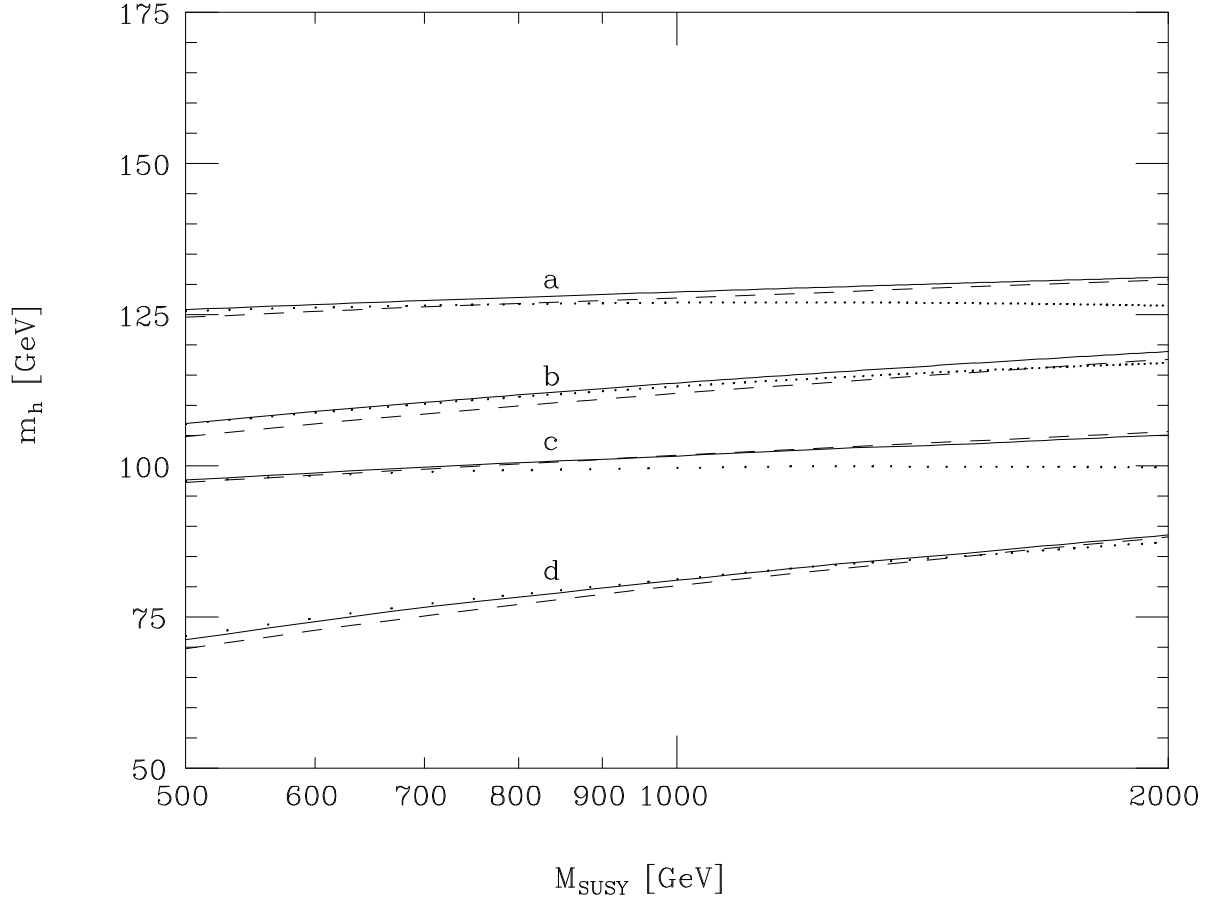


Figure 2: The lightest CP-even Higgs mass as a function of the supersymmetric scale M_{SUSY} , for $M_t = 175$ GeV, and evaluated in the limit of large CP-odd Higgs mass. Solid, dashed and dotted lines are as in Fig. 1. The different sets of curves correspond to the values of \tilde{X}_t and $\tan\beta$ for cases (a) to (d) of Fig. 1.

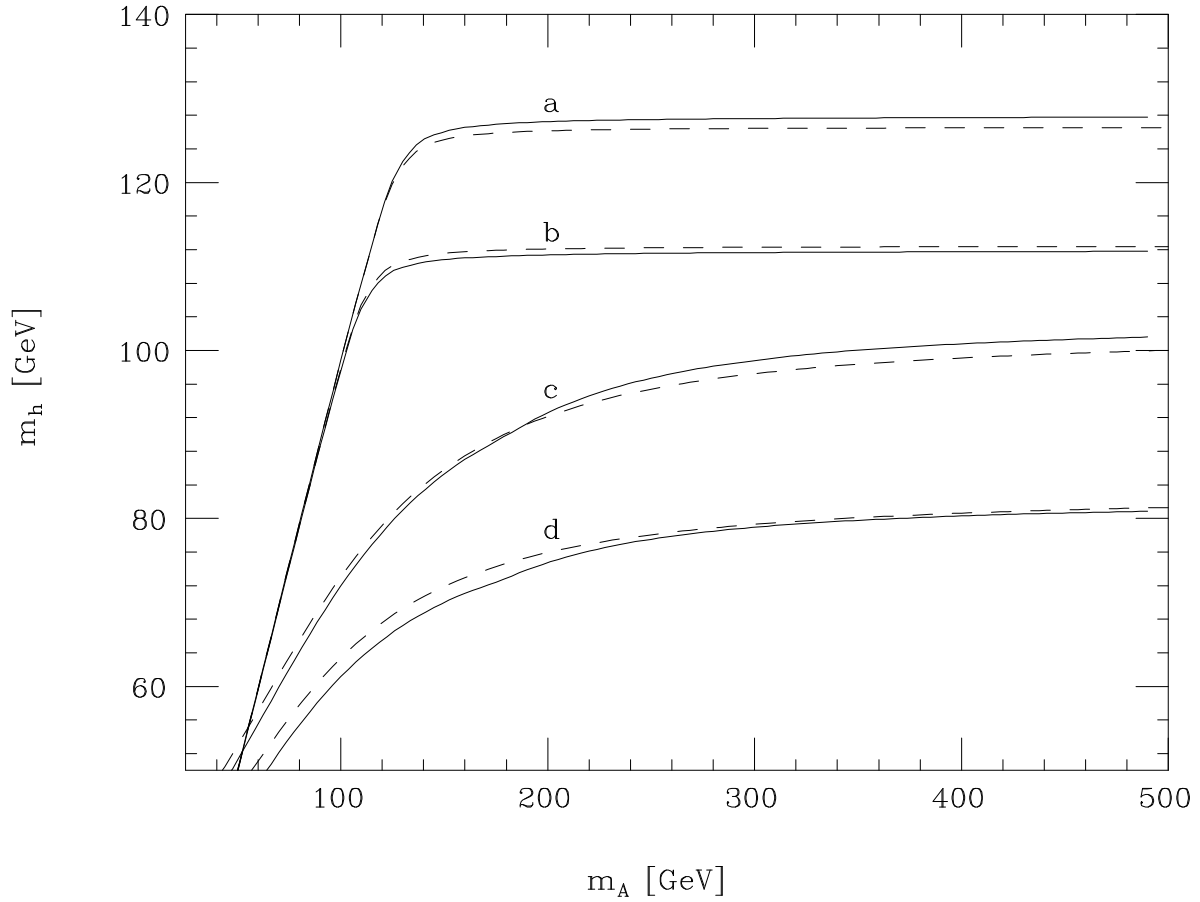


Figure 3: The lightest CP-even Higgs mass as a function of the CP-odd Higgs mass for a physical top-quark mass $M_t = 175$ GeV and $M_{\text{SUSY}} = 1$ TeV, as obtained from the one-loop improved RG evolution (solid lines) and the analytical formulae, Eq. (12), (dashed lines). The four sets of curves correspond to: **a**) $\tan\beta = 15$ with large squark mixing, $X_t = 6$ ($\mu = 0$); **b**) $\tan\beta = 15$ with zero mixing $X_t = \mu = 0$; **c**) the minimal value of $\tan\beta$ allowed by perturbativity constraints for the given value of M_t (IR fixed point), $\tan\beta \simeq 1.6$, with large squark mixing; and, **d**) $\tan\beta \simeq 1.6$ with zero mixing.

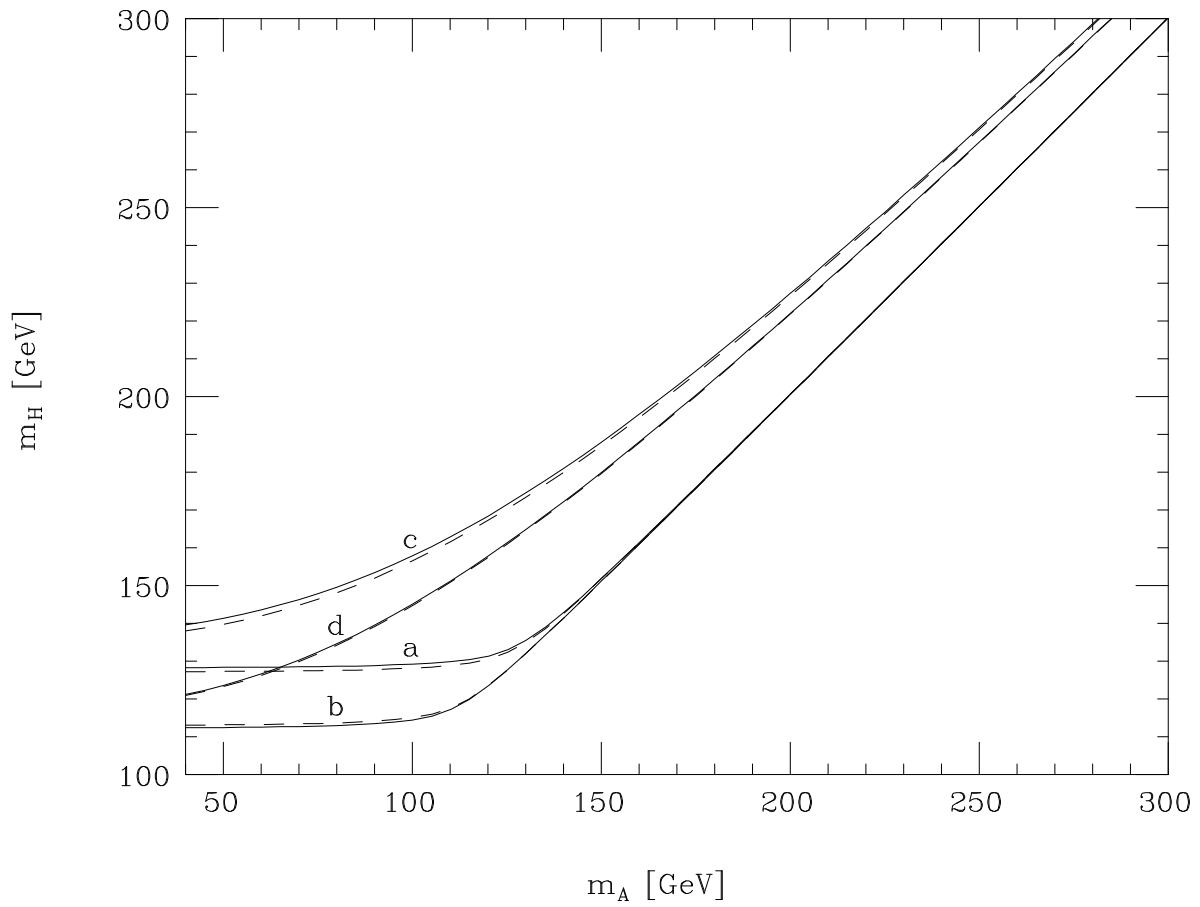


Figure 4: The heaviest CP-even Higgs mass as a function of the CP-odd Higgs mass for the same set of parameters as in Fig. 3.

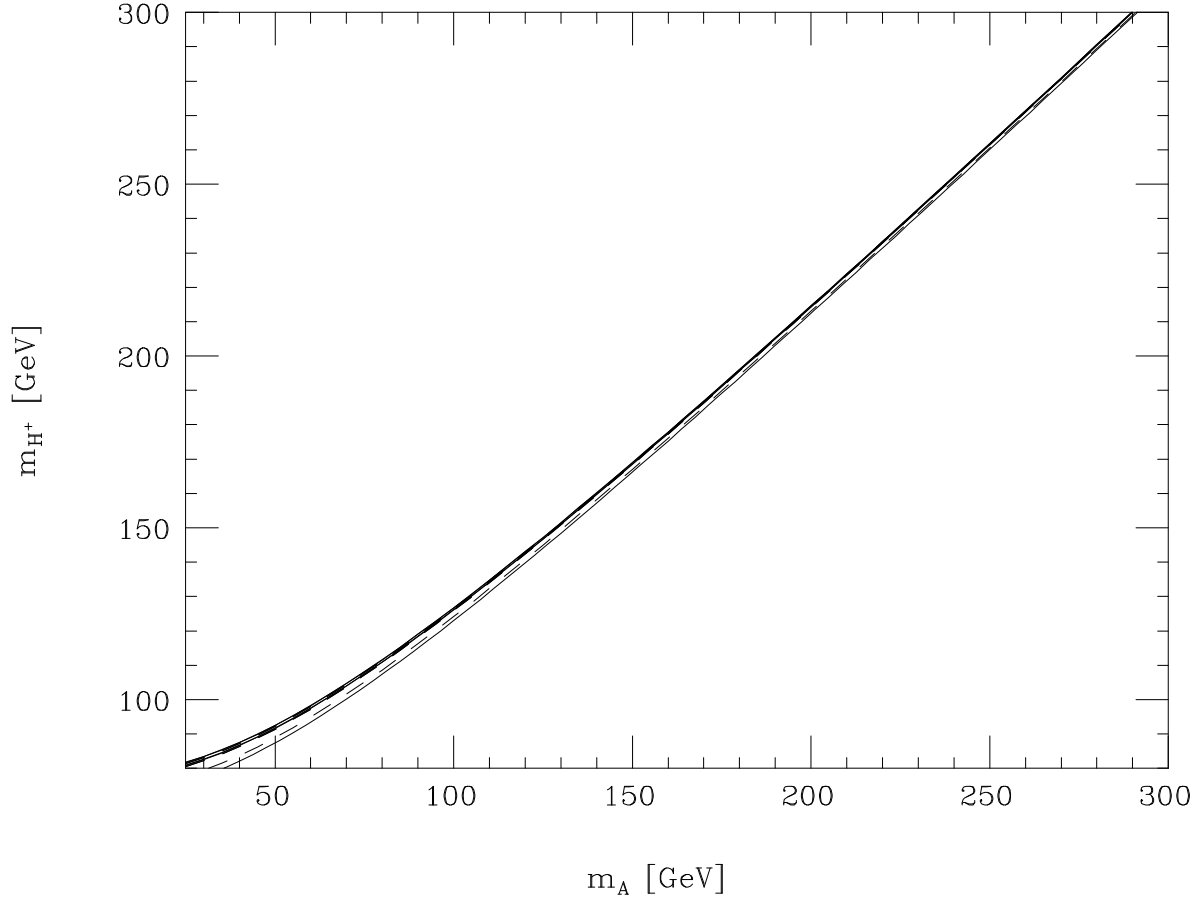


Figure 5: The charged Higgs mass as a function of the CP-odd Higgs mass for the same set of parameters as in Fig. 3 (upper overlapping curves), and for $\mu = 2M_{\text{SUSY}}$ and $\tan\beta = 15$, for which the radiative corrections become observable (solid and dashed lower curves).

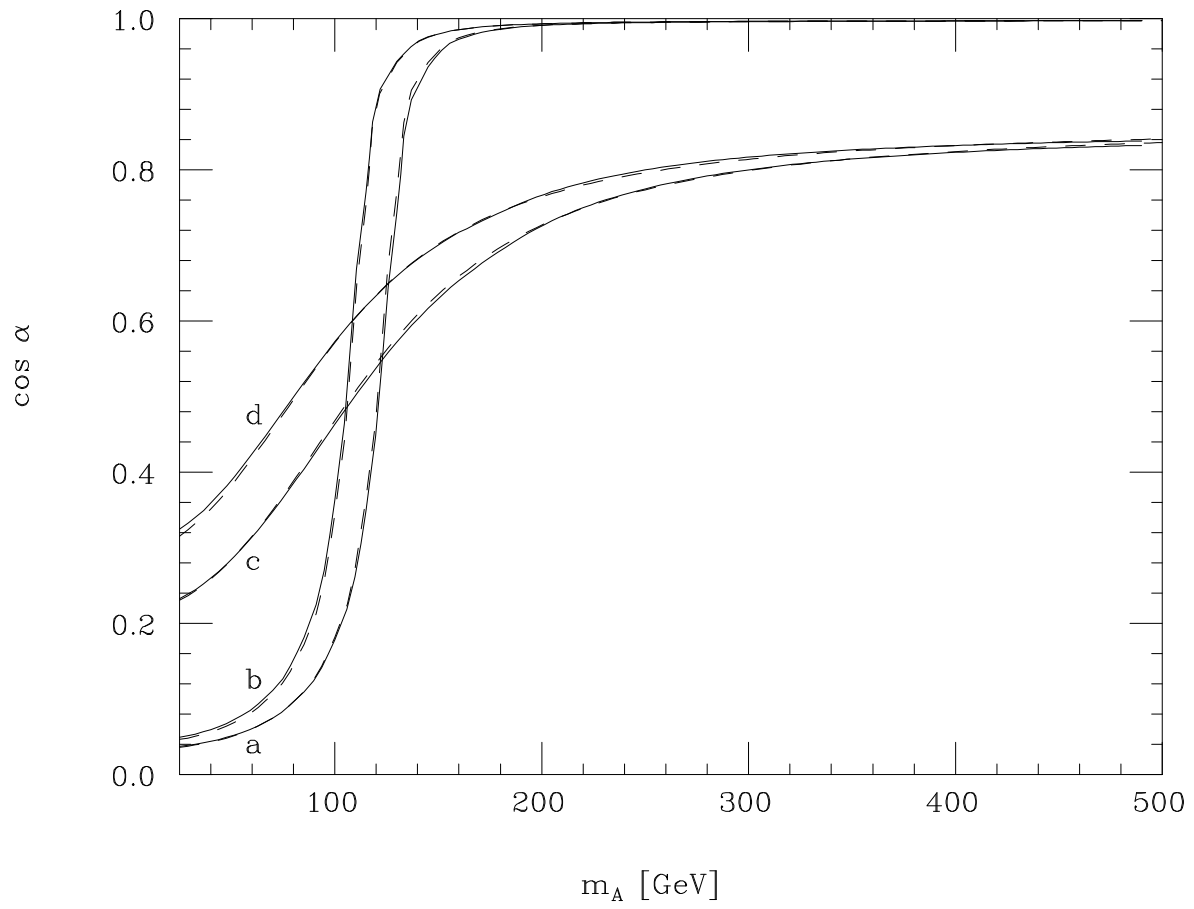


Figure 6: Plot of $\cos \alpha$, as a function of the CP-odd Higgs mass for the same set of parameters as in Fig. 3.

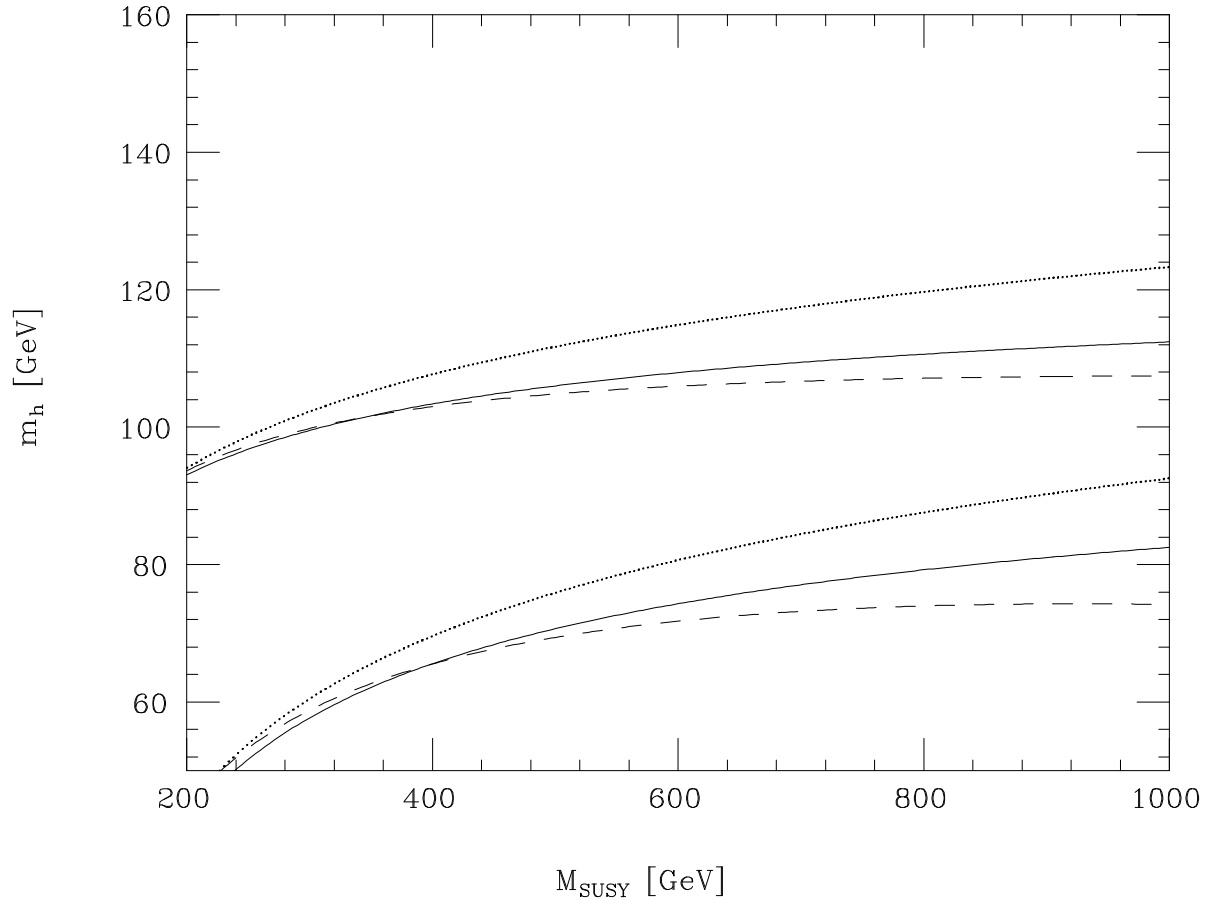


Figure 7: Comparison between the results for the Higgs mass obtained with the analytical approximation (solid lines), the RG improved one-loop MSSM effective potential (dashed lines) and the unimproved one-loop MSSM effective potential (dotted lines), as described in section 4, for $M_t = 175$ GeV, $m_A = M_{\text{SUSY}}$, $m_Q = m_U$, and $A_t = \mu = 0$. The lower set corresponds to $\tan \beta = 1.6$, and the upper set to $\tan \beta = 15$.

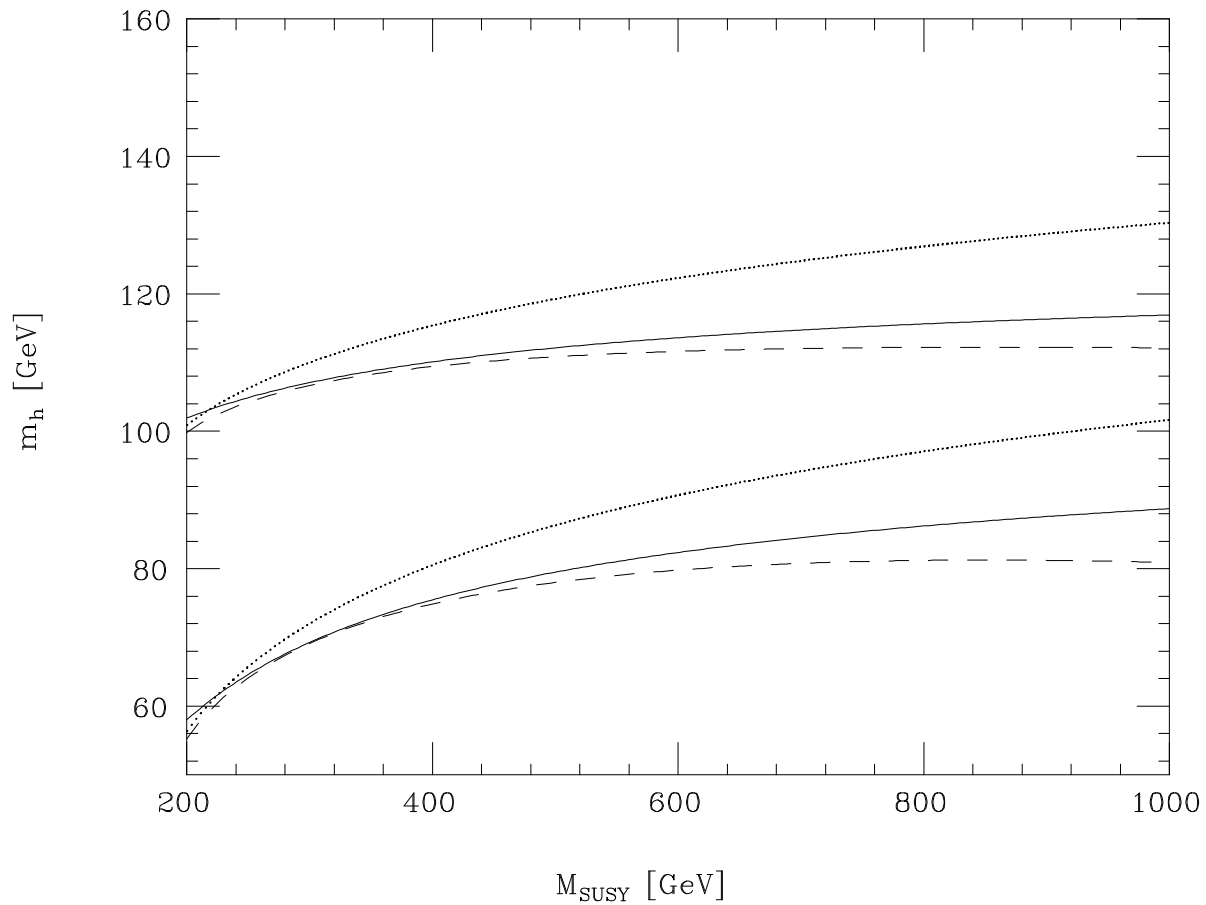


Figure 8: The same as in Fig. 7 but for $A_t = M_{\text{SUSY}}$.